Available online at www.sciencedirect.com
SCIENCE DIRECT
Journal of Magnetic Resonance 179 (2006) 223–233
JMR Journal of Magnetic Resonance
www.elsevier.com/locate/jmr

Effect of impermeable boundaries on diffusion-attenuated MR signal

Astrid F. Frøhlich [a,b,*], Leif Østergaard [a], Valerij G. Kiselev [b]

[a] Department of Neuroradiology, Center of Functionally Integrative Neuroscience (CFIN), University Hospital of Aarhus, Aarhus, Denmark
[b] Medical Physics, Department of Diagnostic Radiology, University Hospital Freiburg, Hugstetterstr. 55, D-79106, Freiburg, Germany

Received 21 July 2005; revised 15 December 2005
Available online 10 January 2006

Abstract

The nonlinear dependence between the logarithm of the diffusion weighted signal, $\ln S$, and the b-value, b, has often been interpreted as a manifestation of two physically distinct compartments, resulting in a biexponential form of the signal. This model fits to experimental data, however, has failed to yield realistic compartment sizes, severely jeopardizing the use of DWI to infer structural information on a cellular level. It has been hypothesized that the biexponential behavior can be attributed to the effect of confining boundaries that restrict diffusion in individual physical compartments. This interpretation is based on the analysis of diffusion in the presence of impermeable interfaces for short diffusion times such that the layer in which diffusion is affected by the boundary is thin as compared with the dimensions of the whole compartment. This model system is analyzed from the point of view of the cumulant expansion of the diffusion-weighted signal that results in a Taylor expansion of $\ln S$ in powers of b. Termination of this expansion to a polynomial form provides an excellent accuracy for small b-factors, but the series diverges for large b. The convergence of the series is studied, yielding a large range of b-values in which the absolute error of terminating the series at the second term remains smaller than 1% relative to the signal magnitude without diffusion weighting. With this accuracy, the signal in the studied model can be described as $\ln S \approx -A \cdot bD + B \cdot (bD)^2$, where the parameters A and B can be expressed in terms of correlation functions of molecular velocity. Fitting of these parameters to the exact signal is more stable than for the three parameters of the biexponential function. This description fails for large b, for which the cumulant expansion diverges. The signal at even larger b-values is proportional to $1/b$, $1/b^{3/2}$, and $1/b^2$ in one-, two-, and three-dimensional systems, respectively.
© 2005 Elsevier Inc. All rights reserved.

Keywords: Diffusion; Restricted diffusion; Cumulant expansion; Biexponential diffusion; Boundaries

1. Introduction

Numerous studies, see, e.g., [1,2] and references therein, give evidence that the normalized diffusion-weighted signal from a single voxel can be described as a weighted sum of two exponential functions

$$S = (1 - w)\exp(-bD_1) + w\exp(-bD_2), \quad (1)$$

where b is the b-value, D_1 and D_2 are two apparent diffusion coefficients, hereafter $D_1 > D_2$ for the definiteness, and w is the volume fraction of the slow-diffusion compartment. The signal in Eq. (1) is commonly termed the biexponential diffusion.

This form of the signal would be exact for samples consisting of two compartments without exchange. The experimentally observed weight of the compartment with slow diffusion is about 20–30% [1,3]. The latter fact presents a serious problem concerning a straightforward interpretation of these compartments as e.g., the intracellular and the extracellular volumes with the slow and the fast diffusion, respectively, since the weight of the intracellular compartment is typically 80% [2,4,5].

A more elaborate model with an exchange term between compartments [6] (the Kärger–Andresko equation) results in a very reasonable signal behavior with time dependence of the apparent diffusion coefficients, but it fails to resolve

* Corresponding author. Fax: +49 761 2703831.
E-mail address: astrid@pet.auh.dk (A.F. Frøhlich).

1090-7807/$ - see front matter © 2005 Elsevier Inc. All rights reserved.
doi:10.1016/j.jmr.2005.12.005

the problem of unrealistically small size of the compartment with slow diffusion [6]. Latour et al. [7] obtained the apparent diffusion coefficient for long times in tissue consisting of densely packed cells, taking into account the finite cell size and permeability of membranes. However, the accuracy of the developed approximation of effective medium remains unclear. The authors did not address the nonlinear dependence between $\ln S$ and the b-factor.

Schwarcz et al. [8] seemingly ruled out the possibility to interpret the biexponential diffusion in relation to the presence of an intracellular compartment. They showed that the biexponential signal decay is observed in the cold-injured mouse brain, where the membranes are disintegrated. The same was shown to be the case for centrifuged red blood cells, having disintegrated membranes. Independence of the weights of two compartments on the actual volume fraction of cells was recently demonstrated by Ababneh and colleagues [9] by a comparison of endemic and normal muscle tissue in a rat model.

These results are in agreement with another interpretation of the biexponential diffusion proposed by Sukstanskii and colleagues [10–12]. They related the "hidden" compartment with slow diffusion to the layers of water adjacent to impermeable or partially permeable membranes which are abundant in biological tissue. This idea is based on a simple model of diffusion with a coefficient D in a slab restricted by two impermeable parallel boundaries. For short times, t, such that the diffusion length, $(Dt)^{1/2}$ is shorter that the slab thickness, L, the apparent diffusion coefficient D_2 does not depend on L and $D_1 \approx D$. The weight, w, of the compartment with low diffusivity scales as $(Dt)^{1/2}/L$.

This model may serve as a basic building block in explaining the behavior of the apparent diffusion coefficient at short times, providing a relation between the signal and the specific surface, σ, (the surface to volume ratio) in porous media [13–15]. In this case the diffusion length should be shorter than the typical pore size. The volume with reduced diffusivity has the weight of the order of $(Dt)^{1/2}\sigma$.

This volume fraction remains small within the validity range of the model, and the problem of unphysiological predictions therefore persists. Nonetheless, it is theoretically attractive by its explanation of the signal being biexponential, and by its impressive accuracy in fitting the expression Eq. (1) to the exact signal [11].

In this paper, we advocate an alternative approach to describe the nonlinear dependence between the logarithm of the diffusion-weighted signal and the b-factor. We refrain from building models of diffusion at the cellular level, adverting instead to an ab initio property of diffusion-weighted signal which is expressed by the following expansion in powers of b:

$$\ln S = -A \cdot bD + B \cdot (bD)^2 + C \cdot (bD)^3 + \cdots, \qquad (2)$$

where D is the diffusion coefficient for free diffusion. It is reasonable to define the apparent diffusion coefficient as the slope of $-\ln(S)$ at $b = 0$. According to this definition, the coefficient A accounts for the time dependence of the apparent diffusion coefficient, $D_{\mathrm{app}} = AD$. In homogeneous media $A = 1$, while B, C, and all higher coefficients turn to zero. The expansion in Eq. (2) follows from an expansion of S in powers of the applied gradient, which is a particular case of the cumulant expansion as discussed below. We shall loosely apply the same term "cumulant expansion" to Eq. (2) in the context of the present paper.

The cumulant expansion, Eq. (2), is in fact a Taylor expansion. Terminating this series provides for a good approximation to the signal when bD is small. This results in a polynomial dependence between $\ln S$ and bD, which diverges after a certain bD-value. Including more terms helps to increase the accuracy only for small bD. For large values, the series diverges. In this case the signal takes a form that cannot be approximated by the exponential of a polynomial and the series in Eq. (2) cannot be applied. The cross-over between the domains of small and large bD can be termed the radius of convergence, following the reason explained below.

To serve as a practical approximation, this radius must be sufficiently large to incorporate measurements with typical experimental b-values. We address this issue using the basic model of diffusion near an impermeable wall in line with a number of previous studies, [11,12,16,17]. The possible applications and restrictions of this basic model is discussed in Section 3. We focus on the simplest measurement sequence with narrow gradient pulses that is used in the q-space imaging and determine the coefficients in Eq. (2). It turns out that the cumulant expansion converges for realistic b-values achievable in human scanners and $\sqrt{Dt} \ll L$. For example, terminating expansion Eq. (2) at the second term for $\sqrt{Dt} = 0.01L$ results in an absolute error which increases with bD and reaches 0.1% of the signal in the absence of diffusion weighting at $bD = 2$. This absolute error remains smaller than 1% for $b < 8$ ms/μm^2. This means that experimental data obtained with b-factors $b < 2$ ms/μm^2, which is typical for human scanners, can be fitted with the two first terms of the expansion in Eq. (2). Such a description involves only two parameters, one of which is the apparent diffusion coefficient D_{app} while the other describes the curvature of the dependence between $\ln S$ and b. A further advantage is that the cumulant expansion of the signal enables to trace the relation between these parameters on one hand and the pulse sequence used as well as the structure of the media investigated, on the other. The latter is represented by the correlation functions of molecular velocity (the cumulants) that may take a rather complicated form. The cumulant expansion of the signal has been discussed in earlier MR studies, e.g., [16,18–21]. We comment on some of these works in Section 3.

The paper is organized as follows: in the next section, we discuss shortly the cumulant expansion of the signal, that gives rise to Eq. (2). The coefficients in Eq. (2) are calculated for the diffusion between impermeable walls in the approximation of narrow gradient pulses. The discussion following in Section 3 focuses on the convergence range

of the cumulant expansion and comparison with the biexponential description of the signal. Mathematical details, which are necessary for the self-sufficiency of the present paper are provided in the Appendix A.

2. Theory

2.1. The cumulant expansion for the signal

The normalized NMR signal from the whole sample, S, can be written in terms of a cumulant expansion in the connected autocorrelation functions of velocity of individual molecules

$$\ln S = \sum_{n=1}^{\infty} \frac{\mathrm{i}^n}{n!} \int u_n(t_1 \cdots t_n) F(t_1) \cdots F(t_n) \mathrm{d}t_1 \cdots \mathrm{d}t_n. \quad (3)$$

Here, $F(t)$ is the integral of the applied gradient, g, to time t:

$$F(t) = \int_0^t g(t_1) \mathrm{d}t_1, \quad (4)$$

where $g(t)$ is the time-dependent gradient of the Larmor frequency, that is applied for the diffusion weighting. The condition of the echo formation is $F(T_E) = F(0) = 0$. A refocusing pulse applied at a time point t_0 is taken into account by alternating $g(t)$ for $t < t_0$. The functions $u_1(t)$, $u_2(t_1, t_2)$, etc., are the connected autocorrelation functions of the velocity of individual water molecules, termed cumulants. The cumulant expansion is discussed in a number of books, see, e.g., [22]. A simple introduction is given in [23]. Note that the quantity $F(t)$ was denoted as $G(t)$ in that paper. Properties of cumulants, termed the connected correlation functions and related quantities are discussed in detail in [24] in the context of field theory.

The sum of all terms of odd orders in Eq. (3) is a pure phase that disappears when the magnitude of the signal is taken, as it is assumed in the following. The sum of terms of all even orders describes the signal attenuation due to the diffusion weighting. This contribution can be expressed in terms of the b-factor using the fact that $b \sim F^2$. The result is given in Eq. (2). This series and its convergence are studied below with the results outlined in Section 1.

2.2. Diffusion between impermeable boundaries

The effect of boundaries is negligible in the MR signal from an infinitely large compartment. A quantification of this effect requires the analysis of a system of finite dimensions. We presently consider the signal from a slab of a homogeneous medium, restricted by two parallel, impermeable planes placed at $x = \pm a$. This system is effectively one-dimensional and we consider only the normal component of the gradient that senses the signal to the effect of boundaries.

The effects of two impermeable interfaces are independent and additive as long as the diffusion length is shorter than the slab thickness: $\sqrt{D\Delta} \ll a$. The accuracy of this approximation will be characterized by a constant $\alpha = \sqrt{D\Delta}/a \ll 1$. We take only the leading term in α into account, which is equivalent to neglecting any cross-effects between the two boundaries.

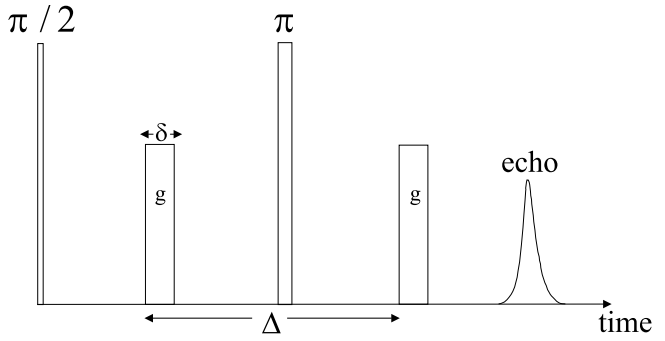

Fig. 1. Sequence of radio frequency and gradient pulses in a pulsed gradient spin-echo (Stejskal–Tanner) experiment. Δ is the duration between the two gradient pulses, δ is the duration of each gradient pulse, and g is the amplitude of these pulses.

The pulsed-gradient spin-echo NMR experiment, Fig. 1, directly measures the Fourier transform of the diffusion propagator, ψ, in the limit of narrow pulses, $\delta \ll \Delta$:

$$S(q,t) = \int \exp(\mathrm{i}q(x - x_0))\psi(x, x_0, t)\mathrm{d}x \frac{\mathrm{d}x_0}{2a}, \quad (5)$$

where $q = g\delta$ and the b-factor of this sequence is $b = q^2\Delta$. The sample thickness, $L = 2a$, which should be replaced by the volume in three dimensions, provides for a normalization $S = 1$ for $g = 0$.

The propagator, ψ, satisfies the equation

$$\frac{\partial \psi(x, x_0, t)}{\partial t} = D \frac{\partial^2}{\partial x^2} \psi(x, x_0, t) \quad (6)$$

with the initial condition

$$\psi(x, x_0, 0) = \delta(x - x_0) \quad (7)$$

and the boundary conditions

$$\psi'|_{x=\pm a} = 0, \quad (8)$$

where the prime denotes the derivative with respect to x. The function $\psi(x, x_0, t)$ is also termed the Green's function of the diffusion equation.

For the free diffusion, the solution to Eq. (6) is a Gaussian function

$$\psi(x, x_0, t) = \frac{1}{(4\pi D t)^{1/2}} \exp\left(-\frac{(x - x_0)^2}{4Dt}\right). \quad (9)$$

In the next section, we calculate the effect of boundaries using two approaches. We use the method of mirror images and the eigenfunction expansion of the diffusion propagator. The former results in very simple calculations while the latter is more universal and commonly used in literature.

2.2.1. Signal attenuation at small b-values

2.2.1.1. Method of mirror images. The Green's function of Eq. (6) in one spatial dimension takes the following form in the vicinity of one boundary:

$$\psi(y,y_0,\Delta)=\frac{1}{\sqrt{4\pi D\Delta}}\left[\exp\left(-\frac{(y-y_0)^2}{4D\Delta}\right)+\exp\left(-\frac{(y+y_0)^2}{4D\Delta}\right)\right]. \tag{10}$$

Here, the distance y, is measured from the position of the boundary: $y=x+a$, $y_0=x_0+a$ near the left plane and $y=x-a$, $y_0=x_0-a$ near the right one. The expression is valid when $y,y_0\ll a$.

The signal in the presence of one boundary can be found by using Eq. (5), with y and y_0 varying between 0 and $2a$. The integration is performed by making a change of variables: $u=y-y_0$ and $v=(y+y_0)/2$. The integral of the first term in Eq. (10) is calculated by first performing the integration over v, while the integral of the second term in Eq. (10) is calculated by first performing the integration over u. Only terms of the orders of a^0 and a^{-1} are taken into account in the calculations. The resulting surface contribution, which is the part of the signal proportional to a^{-1}, is multiplied by a factor of two, to account for the two boundaries present in a slab. This results in

$$S=S_0+S_1+O(\alpha^2), \tag{11}$$

where S_0 and S_1 are given by

$$S_0=\exp(-bD) \tag{12}$$

$$S_1=\frac{\sqrt{D\Delta}}{a}\left[-\frac{1}{\sqrt{\pi}}+\operatorname{erfi}(\sqrt{bD})\exp(-bD)\left(\sqrt{bD}+\frac{1}{2\sqrt{bD}}\right)\right]. \tag{13}$$

Here, $\operatorname{erfi}(x)$ is the error function of an imaginary argument: $\operatorname{erfi}(x)=\operatorname{erf}(\mathrm{i}x)/\mathrm{i}$. $O(\alpha^2)$ stands for corrections of the order α^2 and higher.

Eq. (13) is a particular case of a more general expression for the signal found by Sukstanskii et al. [12] for the case of impermeable walls. The general result was obtained in a different way. It should be noted that the slab thickness in [12] was a rather than $2a$ as it is assumed in the present work. Note a misprint in equation (A.1) in [12].

The surface contribution, S_1, in Eq. (13) can be expanded in a power series in bD giving rise to the following expression for the total signal:

$$S=\exp(-bD)+\frac{\sqrt{D\Delta}}{a}\sum_{l=0}^{\infty}\frac{(l+1)(-1)^l(bD)^{l+1}}{\Gamma(5/2+l)}+O(\alpha^2). \tag{14}$$

The first three terms of this expansion take the form

$$S(b)=1-A_S\cdot bD+B_S\cdot(bD)^2+C_S\cdot(bD)^3, \tag{15}$$

where the coefficients to the first order in α are

$$A_S=+1-\frac{4}{3\sqrt{\pi}}\frac{\sqrt{D\Delta}}{a}, \tag{16}$$

$$B_S=\frac{1}{2}-\frac{16}{15\sqrt{\pi}}\frac{\sqrt{D\Delta}}{a}, \tag{17}$$

$$C_S=-\frac{1}{6}+\frac{16}{35\sqrt{\pi}}\frac{\sqrt{D\Delta}}{a}. \tag{18}$$

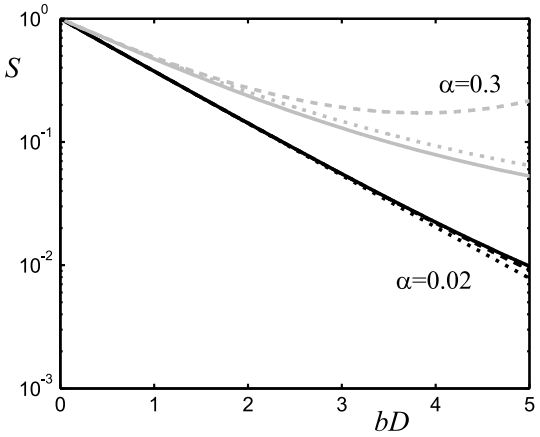

Fig. 2. The exact signal shown as a function of bD for $\alpha=0.02$ (black line) and $\alpha=0.3$ (grey line), along with the cumulant expansion, Eq. (2). The solid lines are the exact signals, Eq. (A.4), the dotted lines the corresponding second-order cumulant expansions, Eq. (2), and the dashed line is the third-order cumulant expansion.

Here, the numerical terms come from the expansion of S_0, Eq. (12), and all terms originated from S_1, Eq. (13), inherit the factor α.

Taking the logarithm of Eq. (14) and re-expanding the series yields finally the signal in the form given in Eq. (2). The expansion coefficients take the following form up to first order in α:

$$A=1-\frac{4}{3\sqrt{\pi}}\frac{\sqrt{D\Delta}}{a},\quad B=\frac{4}{15\sqrt{\pi}}\frac{\sqrt{D\Delta}}{a},$$

$$C=\frac{2}{35\sqrt{\pi}}\frac{\sqrt{D\Delta}}{a}. \tag{19}$$

The case of bulk fluid corresponds to the neglect of boundary effects, which implies $\alpha=0$. In this case the series terminates at the first term with $A=1$, according to the Gaussian nature of diffusion. The deviation of A from unity for finite α describes the known effect of impermeable surfaces. The present result for A agrees with the result of [13], when noting that $1/a$ should be replaced with the surface-to-volume ratio discussed in [13] and an additional factor 1/3 comes from the angular averaging of the gradient in three dimensions. The high accuracy of Eq. (2) for small α is illustrated in Fig. 2. The error made by terminating the cumulant expansion is discussed in more detail in Section 3.

2.2.1.2. Expansion in eigenfunctions. It is instructive to consider another way of solving the problem above. The signal can be found by using the expansion of the diffusion propagator in eigenfunctions of the operator $D\partial^2/\partial x^2$. This method is not so straightforward as above, but it has the advantage of being extendable to semipermeable boundaries with surface relaxation.

The expansion reads

$$\psi(x,x_0,\Delta)=\sum_{n=0}^{\infty}u_n(x)u_n^*(x)\exp(-\lambda_n\Delta), \tag{20}$$

where u_n are the eigenfunctions satisfying the boundary conditions as given in Eq. (8) and λ_n are the corresponding eigenvalues. Calculations that lead to Eq. (14) and Eqs. (11) and (13) are presented in Appendix A.

2.2.2. Signal attenuation at large b-values

The signal at large b-values can be found from Eq. (13) in which the error function takes its asymptotic form

$$\mathrm{erfi}(\sqrt{bD}) = \frac{1}{\sqrt{\pi bD}}\exp(+bD)\left(1+\frac{1}{2b}\right). \tag{21}$$

This results in the following form of the signal:

$$S(bD) \approx \frac{\sqrt{D\Delta}}{\sqrt{\pi}a}\cdot\frac{1}{bD}. \tag{22}$$

The same expression can be obtained via the eigenfunction expansion by neglecting ξ_n and ζ_n in the denominator of Eq. (A.4) and evaluating the series in Eq. (A.4) in its integral limit.

The total signal in Eq. (22) is dominated by the contribution of the molecules that experience the confining effect of the boundary. They are less mobile than in the bulk and their contribution to the signal is less suppressed. The dependence on the parameters in Eq. (22) can be recovered by estimating the signal using Eq. (5). The main contribution to the signal comes from a region adjacent to the boundary with the thickness of the order of $1/q$. In this region, the Green's function is of the order of $1/\sqrt{D\Delta}$. Accordingly, the double integration results in $S \sim (q^2\sqrt{D\Delta})^{-1}$ in agreement with Eq. (22). The relative smallness of the bulk contribution defines the applicability range of Eq. (22) as

$$\exp(-bD) \ll \frac{\sqrt{D\Delta}}{a}\cdot\frac{1}{bD}. \tag{23}$$

The signal behavior at large b is illustrated in Fig. 3 for three different values of α. At $bD \approx 10$ the asymptotic form sets up. Such a strong diffusion weighting is achievable in animal scanners and spectrometers, see for example [25], in which b-values up to 15 ms/μm^2 are reported.

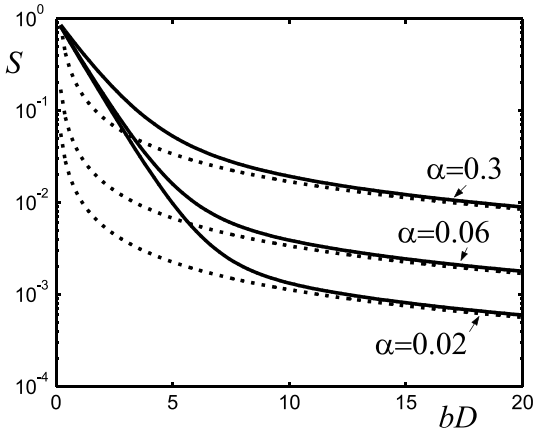

Fig. 3. The signal, Eq. (11), as a function of bD, for large b-factors for three different values of α (solid lines). Dotted lines show the asymptotic form, Eq. (22), for $bD \gg 1$.

The above result can be easily generalized for three-dimensional systems. The applied gradient, if not orthogonal to the boundary, results in the conventional signal attenuation due to the diffusion in the lateral directions. In three dimensions Eq. (22) is replaced with

$$S_{3d}(bD) = \int S(bD\cos^2\theta)\exp(-bD\sin^2\theta)\frac{\sin\theta}{2}\mathrm{d}\theta. \tag{24}$$

Here, S is defined in Eq. (22), in which $1/a$ is replaced with $\sigma/2$. θ is the tilt angle of the gradient and the integration performs the averaging over all possible orientations in a statistically isotropic sample. The integral at large bD is dominated by the saddle points at $\theta = 0$ and $\theta = \pi$ with the result

$$S_{3d}(bD) \approx \frac{\sqrt{D\Delta}}{4\sqrt{\pi}(bD)^2}\cdot\sigma. \tag{25}$$

Analogously, the signal from two-dimensional systems takes the form

$$S_{2d}(bD) \approx \frac{\sqrt{D\Delta}}{2\pi(bD)^{3/2}}\cdot\sigma. \tag{26}$$

3. Discussion

We have advocated the cumulant expansion for the diffusion-weighted signal, Eq. (2), and obtained all terms in the expansion of the signal in powers of the b-value for the pulsed-gradient spin-echo experiment in the approximation of narrow pulses, Eq. (14). The re-expansion of the logarithm of the signal can be easily extended to give any reasonably large number of terms beyond the first three ones given in Eq. (19). In this section, we discuss the convergence of the expansions obtained, their relation to the biexponential model, give a brief overview of similar approaches in the current literature and finally discuss limitations of the model used.

3.1. On the convergence range of the cumulant expansion

A theorem of complex analysis states that an arbitrary smooth analytical function can be expanded in a Taylor series in a vicinity of a given point in the complex plane of its argument. In our case the argument is bD and the expansion point is $bD = 0$. The Taylor expansion converges in the complex plane of bD in a circle with a radius restricted by the nearest singularity or branching point of the original function. This radius, which is termed the radius of convergence, can take values from zero to infinity depending on the specific function.

Consider first an illustrative example of a function $y = 2-\exp(-x)$ which converges for any x. We can re-write y as $\exp(\ln(y))$ and then expand the logarithm, $\ln(2-\exp(-x))$, to simulate the cumulant expansion. In

this case the convergence radius is limited by the singularity of y at $x = -\ln(2)$. In particular, the series diverges for $x > \ln(2) \approx 0.69$, although the function has no singularity at positive arguments. The difference in the radius of convergence results in two different types of behavior of the terminated series as illustrated in Figs. 4A and B. For the infinite radius of convergence, Fig. 4A, accounting for more terms in the Taylor expansion results in a larger interval in which the function is well approximated by the terminated series. In contrast, the terminated series can never approximate the function beyond the radius of convergence as it is illustrated by Fig. 4B.

The same two types of convergence are met in the diffusion-weighted signal, Eqs. (2) and (14) as illustrated in Fig. 4C. The expansion of the signal in velocity correlators, Eq. (14), converges for all values of bD due to the presence of the Gamma function in the denominator. In contrast, the cumulant expansion, Eq. (2), shows a pattern that is peculiar to a finite radius of convergence, due to the re-expansion of $\ln S$.

This radius can be estimated by searching for zeros of $S(bD)$ given in Eq. (11) in the complex plane of bD. The result of such a search, which was performed numerically, is shown in Fig. 5. For $\alpha = 0.02$ the signal has a zero point at $bD = -6.362 \pm 3.856i$, giving a convergence radius of $(bD)_c = 7.44$. This value depends on α (Fig. 6). The quantity $(bD)_c$ is an approximation to the radius of convergence of the cumulant expansion in the first order in α. Taking the logarithm of the signal produces an infinite number of terms of higher orders in α. These terms are neglected in Eq. (2) which is equivalent to a subtraction of a function of α and bD that is proportional to α^2. The data shown in Fig. 4 agree with the above estimate for $\alpha = 0.02$.

The behavior of the signal for all small values of α is illustrated in Fig. 6. The cumulant expansion has a larger applicability range for small α. The cross-over to the regime of large b takes place at logarithmically large bD as $\alpha \to 0$.

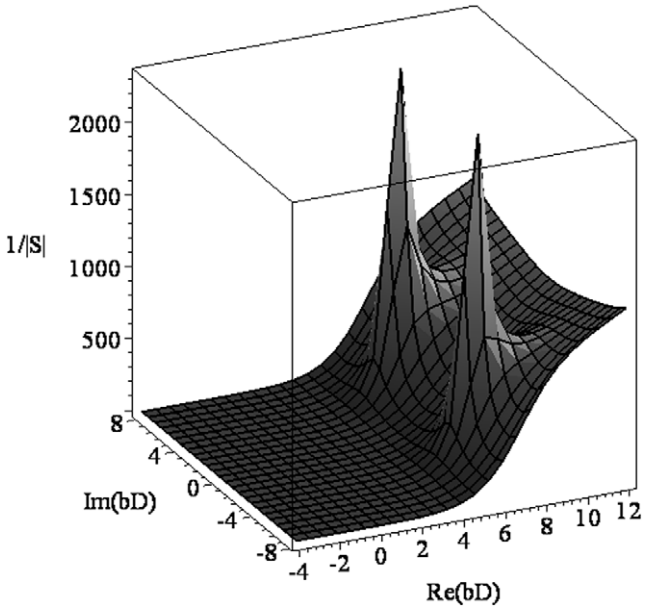

Fig. 5. $1/|S|$ (from Eq. (11)) in the complex plane of bD, for $\alpha = 0.02$. $1/|S|$ is symmetric around the real axis, due to the property $S(bD)^* = S(bD^*)$, where the star denotes the complex conjugation. The signal is a real positive decreasing function of bD on the real axis. It has a zero point at $-6.362 \pm 3.856i$ (found numerically), which can be seen as the divergence in $1/|S|$. This restricts the convergence radius in the expansion of Eq. (2) to $\sqrt{6.362^2 + 3.856^2} = 7.44$.

3.2. Relation to the biexponential model

According to Sukstanskii and colleagues [11], the model of biexponential diffusion, Eq. (1), describes the signal from a slab restricted by two impermeable walls extremely well ($\chi^2 < 10^{-9}$). This model inspires the interpretation of real experimental data as the effect of restricted diffusion. We argue, however, that the conclusion about the biexponential nature of diffusion in this basic model cannot be drawn if the signal is determined with a finite accuracy of the order of the typical noise level in in vivo experiments.

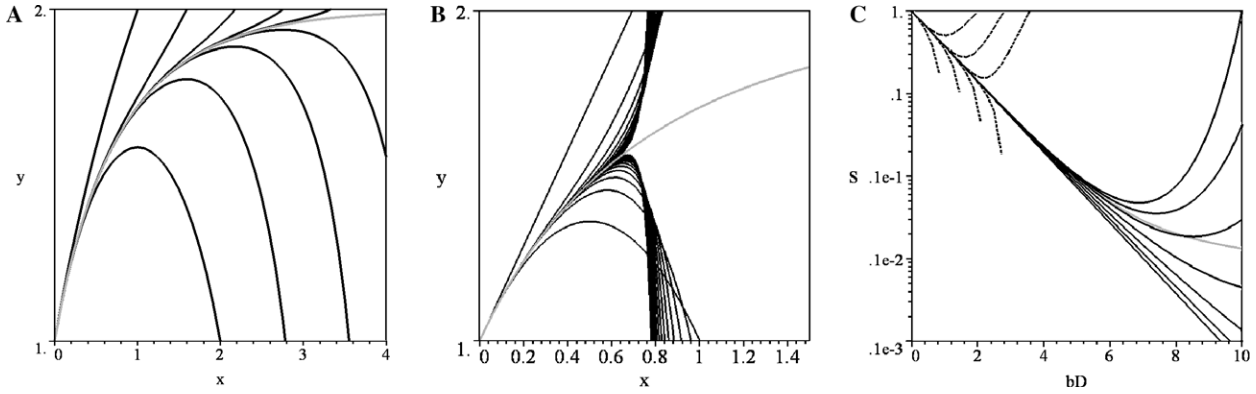

Fig. 4. Two examples of convergence to compare with the signal, S, shown as a function of bD. (A) Taylor expansion of the function $y = 2 - \exp(-x)$ (grey line). Black lines represent its terminated Taylor expansion including from two to ten terms. (B) Taylor expansion of the function $\exp(\ln(2 - \exp(-x)))$ (see text) with the same meaning of the lines. (C) The exact diffusion-weighted signal, Eq. (A.4) (grey line) for $\alpha = 0.02$. The black dashed curves show the expanded signal, Eq. (14), to increasing order in bD. Note a similarity to (A). The black solid curves represent the terminated cumulant expansion, Eq. (2), to increasing order in bD. Note a similarity to (B).

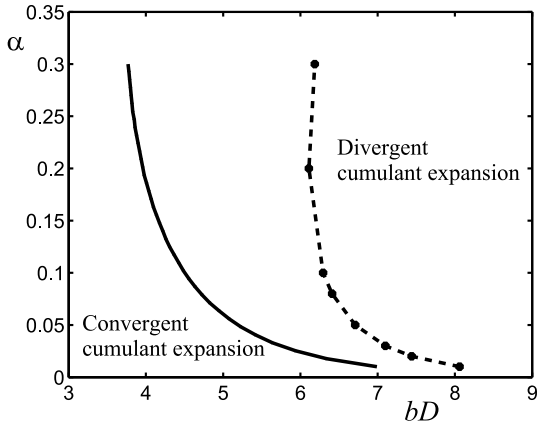

Fig. 6. Regions in the parameter plane (α, bD) that are relevant for the convergence of the cumulant expansion. The first two terms of the cumulant expansion, Eq. (2), provide a good relative accuracy in the region to the left of the solid line. The line is selected to show the point for which this approximation deviates two-fold from the exact signal, Eq. (A.4). The line shape is well described by the formula $\alpha = 5.34e^{-0.9bD}$ for $bD > 4$. The points connected with the dashed line show the estimation for the radius of convergence of the cumulant expansion as discussed in the text. Accounting for more terms in the expansion can help to increase the accuracy in the region between the two lines. The signal for large α ($\alpha > 0.3$) is not concave any more [11] and the present model is not applicable.

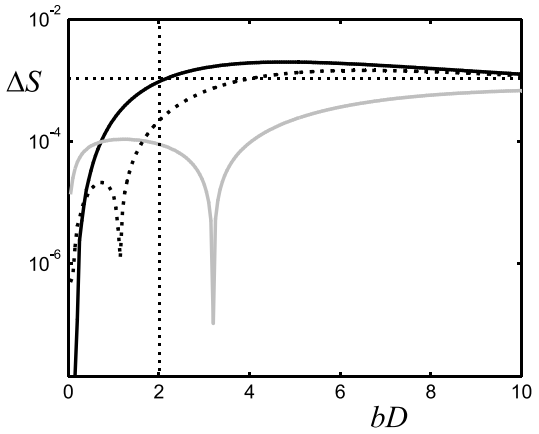

Fig. 7. The absolute value of the error shown as function of bD for $\alpha = 0.02$. The error is defined as the absolute difference between the exact signal, obtained by numerical summation of the series in Eq. (A.4), and the approximated signal. The second and third order of the cumulant form are shown by the black solid curve and the black dotted curve, respectively. The grey solid curve corresponds to the biexponential fit performed by Sukstanskii et al. [11], which should only be evaluated in the interval $0 < bD < 2$, in which the fitting was performed.

This can be understood as follows: any smooth function can be represented by the coefficients of its Taylor expansion. Knowledge of all coefficients is equivalent to the knowledge of the original function, while incomplete determination of the coefficients causes an error in the sum of the series. In the context of the present discussion, the biexponential function, Eq. (1), can be cast into the generic form of Eq. (2). Recognition of this function as biexponential would require either a determination of a sufficiently large number of coefficient in its Taylor expansion or a good accuracy of the biexponential approximation beyond the convergence range of the series.

Fig. 7 shows that this is not feasible for a typical noise level of the order of 1% relative to the signal at $b = 0$. The *absolute* error in the signal is addressed in view of the noise which is additive in real measurements. This error, of both the fitted biexponential function and its cumulant expansion terminated at the second term, remains smaller than 1% in a large range of b-values. This implies that the coefficients A and B in Eq. (2) are the only practically relevant parameters, while the rest of the Taylor expansion for $\ln S(b)$ is irrelevant. For $\alpha = 0.02$, reduction of noise down to the level of 10^{-3} would be marginally sufficient for more terms to become significant, as shown in Fig. 7. The *relative* error of the second-order cumulant expansion increases with bD. Still, it remains small in a reasonably large range of parameters, for example it is smaller than 10^{-2} for $bD < 3$ (for $\alpha = 0.02$). Note that the cumulant expansion that accounts for the coefficients A and B in Eq. (2) results in an increasing signal for $b > A/2B$ which gives $b > 160$ for $\alpha = 0.02$ and $b > 8$ for $\alpha = 0.3$. These values are far beyond the radius of convergence. The cumulant expansion is more accurate in the limit of small b-values in agreement with its exact mathematical origin.

We thus conclude that the biexponential function, Eq. (1), is superfluous to describe the diffusion-weighted signal from a rectangular compartment. There are only two parameters, A and B in Eq. (2) that can be reliably determined from experimental data acquired with realistic accuracy. This relevant part of the signal takes the following form in terms of the original parameters of the biexponential function, Eq. (1):

$$\ln S \approx -b\bar{D} + \tfrac{1}{2}b^2\left[w_1(D_1 - \bar{D})^2 + w_2(D_2 - \bar{D})^2\right]. \qquad (27)$$

Here, $w_2 = 1 - w_1$, $\bar{D}$ is the mean value of the diffusion coefficient, $\bar{D} = w_1 D_1 + w_2 D_2$ and the term in the brackets can be recognized as the variance of the diffusion coefficient between the two pools. This representation enables a comparison of our analytical results with the results of fitting the biexponential model to the signal calculated numerically which was performed in [11]. The data from [11] were cast into the form Eq. (2) by use of Eq. (27). The results presented in Table 1 indicate a good agreement between the studies.

Table 1
Comparison of the coefficients A_S, B_S, and C_S in the signal in Eq. (14) with numerical calculations of [11]

		$\alpha = 0.02$	$\alpha = 0.3$
A_S	Present study	−0.9849	−0.7743
	Sukstanskii et al. [11]	−0.9847	−0.7863
B_S	Present study	0.4880	0.3195
	Sukstanskii et al. [11]	0.4876	0.3246
C_S	Present study	−0.1615	−0.0893
	Sukstanskii et al. [11]	−0.1613	−0.0908

Table 2
Parameters found from a biexponential fit to the exact result, Eq. (14), represented with 40 points in the interval $0 < bD < 2$ for $\alpha = 0.02$

Biexponential fit				Cumulant expansion	
D_1	D_2	w	χ^2	A	B
0.9933	0.3030	0.0121	4.3701×10^{-11}	0.9849	0.0028
0.9915	0.2110	0.0086	1.0569×10^{-8}	0.9847	0.0026
0.9900	0.1012	0.0060	2.7892×10^{-8}	0.9846	0.0024

The three data lines correspond to three different sets of initial parameters. The parameters of the biexponential fit show large variations in spite of the high accuracy of fitting. The coefficients of the cumulant expansion are more stable as discussed in the text.

In general, fitting the three parameters of the biexponential function to data, which are described by only two parameters, may cause large fluctuations in the fitting results which would be driven by the noise or the initial guess. Such fluctuations would be correlated to preserve the two combination of parameters in Eq. (27) which are actually fixed by the data. This effect is illustrated in Table 2. The noise-free theoretical curve, Eq. (11), was represented with 40 points in the interval $0 < bD < 2$ for $\alpha = 0.02$, and fitted with the biexponential function with three different sets of initial parameters. The parameters of the cumulant expansion, Eq. (2), were calculated according to Eq. (27) from the results of fitting. In all cases, very accurate fits were obtained with a standard deviation between the data and the fitted function smaller than 2.6×10^{-5}. In spite of this impressive accuracy, the small diffusion constant and the corresponding weight vary three- and two-fold, respectively. In contrast, the coefficients of the cumulant expansion are stable. Similar results were obtained with Gaussian noise added prior to the fitting (data not shown).

3.3. Overview of the diffusion weighted signal

It is a well-known fact that diffusion-weighted signal for short times from samples with impermeable interfaces is corrected proportionally to the specific surface of the sample [13,26]. According to the present results, the total signal as a function of the b-factor shows two different regimes which will be referred to as the small and large b-values (Fig. 8). The cross-over between them is related to the convergence radius of the cumulant expansion.

The signal for small b-values decreases exponentially as a function of bD. Its form is described by the cumulant expansion, Eq. (2). Both this expansion and the fitting with the bi-exponential function, Eq. (1), provide for a good accuracy.

The cumulant expansion is not applicable in the cross-over region and for large b-factors the signal is proportional to an inverse power of bD, Eq. (22) and Eqs. (25) and (26). Note that the biexponential function is sufficiently flexible to be fitted to the signal in a wide range of b-values as illustrated in Fig. 8. The systematic deviation from the exact result reminds about its incorrect functional form in the domain of large b-factors.

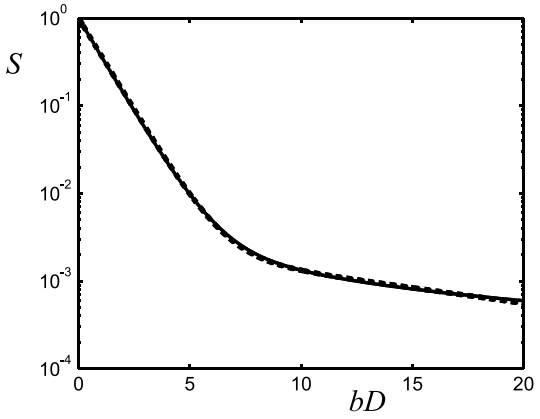

Fig. 8. The signal (solid curve) as a function of bD for $\alpha = 0.02$ along with the biexponential fit (dotted curve), Eq. (1) The fitted parameters are $D_1 = 0.9656$, $D_2 = 0.0819$, and $w = 0.0029$.

3.4. Cumulant expansion in MRI literature

The cumulant expansion is well known in physics and mathematics and has to some extend been reflected in the MRI literature. Several groups have used related approaches for modelling the diffusion-weighted signal.

The representation of the diffusion-weighted signal as an exponential function of a second-order polynomial, which is equivalent to Eq. (2) terminated at the second term, was proposed by Yablonskiy and coauthors [27]. It was demonstrated that this function fits well in vivo data. This form of the signal was derived from an assumption that the signal in the form $\exp(-bD)$ gets weighted with a probability distribution of the diffusion coefficient, $P(D)$. A narrow Gaussian distribution resulted in the second-order polynomial in the exponent. This approach can be generalized by noting that the whole series in Eq. (2) can be obtained as the cumulant expansion for arbitrary $P(D)$. The drawback of this model is the unclear meaning of the distribution $P(D)$, which was thought of as a function of time for any given spin packet [27]. From our point of view, this description can be applied self-consistently to the only model that describes a medium consisting of many large homogeneous compartments. In this case $P(D)$ would describe the distribution of compartments. Apparently, such a model can hardly be applied to the cellular structure of brain tissue with the typical cell size of the order of 10 μm.

Mitra and colleagues [16] studied the cumulant expansion, and found the quadratic term in b-value in the limit of long times for three different geometries. The authors concluded that this term can be a very sensitive probe of microgeometry.

Jensen et al. [20] discussed the deviation of diffusion from a Gaussian distribution and derived the corresponding corrections to $\ln S$ for the case of narrow gradient pulses. Their main equation corresponds to Eq. (2) terminated at the second term and generalized for three dimensions. The authors have shown that the second-order term in b is rather sensitive to the anisotropy of diffusion.

Cohen and Assaf [25] compared the q-space analysis with the biexponential fit. They found a much larger error in the parameters of their biexponential fit than in the height and the width of the displacement distribution, which was calculated straightforwardly (Fig. 20 in the original paper). This can be explained by the redundancy of the biexponential function, Eq. (1), as discussed above.

In [18] Stepišnik studied the second-order term of the cumulant expansion which is proportional to bD. He discussed the possibility to measure the velocity autocorrelation function by using oscillating gradients. This idea was realized later by Schachter, Does, and colleagues [28,29]. In 2004, Stepišnik [21] studied the cumulant expansion for large α-values, and concluded for this case that higher-order terms bring small corrections to the Gaussian phase approximation, which is equivalent to keeping only the first term in the cumulant expansion, Eq. (3).

3.5. Restrictions of the model

The model considered in this study provides an illustration to the discussion of the general properties of the diffusion-weighted signal. It becomes adequate in the limit of short diffusion times such that the diffusion length $\sqrt{Dt}$ is much smaller than the characteristic size of the mesoscopic structure in the medium. The curvature of realistic boundaries contributes a subleading term at short times [14].

Sukstanskii and colleagues [12] discussed the applicability of the present model to the diffusion measurements in the human brain. Cells in the brain have a size distribution above $\sim$1 μm. The diffusion time should be as short as $\sim$1 ms to fulfill the criterium $\alpha \ll 1$ when $D \sim 1\ \mu m^2/ms$ is used as the lower limit on the "bulk" diffusion coefficient. Such small diffusion times are marginally reachable (see e.g., [29]). Latour et al. [7] achieved a diffusion time of 3 ms and successfully found the surface-to-volume ratio of packed red blood cells by extrapolation to zero time. The typical diffusion times used in MR are significantly longer, of the order of $\sim$20 ms. Accordingly, the effects considered here are relevant for cellular structure larger than 15 μm. This minimal size is smaller for the diffusion of some brain metabolites that have a much smaller diffusion constant.

In the present study, the boundaries were assumed to be impermeable for diffusing molecules. The effect of finite permeability of cellular membranes was discussed in [11,12]. It can be estimated in terms of a characteristic time, D/κ^2, where κ is the permeability. The membrane can be well approximated as impermeable as long as this time is longer than the diffusion time. For a typical permeability of $10^{-2} - 10^{-1}$μm/ms [12], this requirement is less restrictive than the requirement of $\alpha \ll 1$.

The effect of surface relaxation was not taken into account in the present model. It results in terms which are proportional to time [14] at $t \to 0$. Such terms are smaller than the leading one of the order of $\sqrt{Dt}$ which is in the focus of the present study.

In the present work, we assumed a negligible duration of the gradient pulses. This assumption can hardly be met in in vivo measurement with strong diffusion weighting. On the other hand, the signal dependence on the applied gradient includes two successive integrations, Eqs. (3) and (4). This suggests that the signal should not depend significantly on the details of the gradient pulse shape.

4. Conclusion

The present study focuses on diffusion near confining boundaries. This model underlies a widely shared interpretation of complex diffusion in the human brain as being biexponential. An alternative description is provided by the cumulant expansion of the logarithm of the diffusion-weighted signal that takes the form of a power series in bD. We find explicitly the first terms of this expansion in the narrow pulse approximation and show that the series converges in the range of practically important b-values. In this range, it can be approximated by its first two or three terms which provide for a very good approximation to the exact result similar to the biexponential description.

We show that the limitation of realistic experimental accuracy helps to resolve the problem of choice between one of these two ways of mathematical description of the signal. Only the two first terms of the Taylor expansion of the biexponential function can be reliably determined from experimental data at a noise level of around 1%. Keeping only these terms is identical to using the cumulant expansion. The rest of the Taylor series for the biexponential function is irrelevant. The biexponential function with its three parameters is thus superfluous for fitting such experimental data. This results in large correlated fluctuations in the fitted parameters which are driven by noise and the initial guess. Further advantage of the cumulant expansion is the better understanding of its relation to the microscopic structure.

The signal at large b-values cannot be described by the cumulant expansion that diverges for large bD. The signal in this domain is proportional to an inverse power of bD. The biexponential function can still be used to fit the data, although a systematic deviation from the exact result is manifest.

The system considered in this study cannot serve as a realistic model for diffusion measurements in the brain. It

rather helps to insight in those properties of the signal that follow from basic physics and are thus inherent to a large class of systems. It remains a challenging unresolved problem to find the morphological correlates of diffusion-weighted signal in biological tissue.

Acknowledgments

We thank A.L. Sukstanskii and D.A. Yablonskiy for a useful discussion and P. Gall for helping to prepare the manuscript. We are grateful to the Danish National Research Foundation's Center of Functionally Integrative Neuroscience (A.F.F. and L.Ø.), The Danisch Medical Research Council (L.Ø.) and Deutsche Forschungsgemeinschaft (V.G.K.) for supporting this work. A.F.F. appreciates hospitality of the staff at Medical Physics, University Hospital Freiburg.

Appendix A

The Green's function is conveniently expressed in terms of eigenfunctions of the operator $D\partial^2/\partial x^2$, Eq. (6)

$$\psi(x,x_0,\Delta)=\sum_{n=0}^{\infty}u_n(x)u_n^*(x)\exp(-\lambda_n\Delta), \tag{A.1}$$

where the eigenfunctions $u_n(x)$ form an orthogonal complete set

$$\int_V \mathrm{d}x\,u_n(x)u_m(x)=\delta_{n,m},\quad \sum_{n=0}^{\infty}u_n(x)u_n(x_0)=\delta(x-x_0) \tag{A.2}$$

and obey the boundary conditions given in Eq. (8).

For diffusion between the parallel planes, the expansion in eigenfunctions for the Green's function takes the form

$$\psi(x,x_0,\Delta)=\frac{1}{2a}+\frac{1}{a}\sum_{n=1}^{\infty}\exp\left(-\frac{\xi_n^2D\Delta}{a^2}\right)\cos\left(\frac{\xi_n x}{a}\right)\cos\left(\frac{\xi_n x_0}{a}\right)+\frac{1}{a}\sum_{n=0}^{\infty}\exp\left(-\frac{\zeta_n^2D\Delta}{a^2}\right)\sin\left(\frac{\zeta_n x}{a}\right)\sin\left(\frac{\zeta_n x_0}{a}\right), \tag{A.3}$$

where the eigenvalues ξ_n and ζ_n are determined by $\sin(\xi_n)=0$ and $\cos(\zeta_n)=0$. In the case of free diffusion, $a\to\infty$, the series in Eq. (A.3) can be approximated by integrals and ψ takes the well-known Gaussian shape, Eq. (9). By performing the Fourier transform of Eq. (A.3), the signal can be written as [17]

$$S(q,\Delta)=2\sum_{n=0}^{\infty}\exp\left(-\frac{\xi_n^2D\Delta}{a^2}\right)\frac{(qa)^2\sin^2(qa)}{\left((qa)^2-\xi_n^2\right)^2}-\frac{\sin^2(qa)}{(qa)^2}+2\sum_{n=0}^{\infty}\exp\left(-\frac{\zeta_n^2D\Delta}{a^2}\right)\frac{(qa)^2\cos^2(qa)}{\left((qa)^2-\zeta_n^2\right)^2}. \tag{A.4}$$

This expression can be expanded in powers of q, by using the following formal series:

$$\frac{1}{\left[(qa)^2-\xi_n^2\right]^2}=\sum_{l=0}^{\infty}\frac{(l+1)(qa)^{2l}}{\xi_n^{4+2l}}. \tag{A.5}$$

The summation over n in the first series in Eq. (A.4) can be performed as follows. A series of this type can be evaluated as an integral to the first order in α provided a weak dependence on n. To this end we subtract and add the first $l+1$ terms of the Taylor expansion of the exponential function:

$$\sum_{n=0}^{\infty}\frac{1}{\xi_n^{4+2l}}\exp\left(-\frac{\xi_n^2D\Delta}{a^2}\right)=\sum_{n=0}^{\infty}\frac{1}{\xi_n^{4+2l}}\left[\exp\left(-\frac{\xi_n^2D\Delta}{a^2}\right)-\sum_{p=0}^{l+1}\frac{(-1)^p}{p!}\left(\frac{\xi_n^2D\Delta}{a^2}\right)^p\right]+\sum_{n=0}^{\infty}\frac{1}{\xi_n^{4+2l}}\sum_{p=0}^{l+1}\frac{(-1)^p}{p!}\left(\frac{\xi_n^2D\Delta}{a^2}\right)^p \tag{A.6}$$

and analogously for the second series in Eq. (A.4). The signal can be written from now on as $S=S_1+S_0$, where S_1 is the part of the signal in Eq. (A.4) coming from the first sum in Eq. (A.6). S_0 is the part of the signal in Eq. (A.4) coming from the second sum in Eq. (A.6) and including the term $-\sin^2(qa)/(qa)^2$ in Eq. (A.4).

Evaluation of S_1 as an integral is performed as follows:

$$\sum_{n=0}^{\infty}\frac{1}{\xi_n^{4+2l}}\left[\exp\left(-\frac{\xi_n^2D\Delta}{a^2}\right)-\sum_{p=0}^{l+1}\frac{(-1)^p}{p!}\left(\frac{\xi_n^2D\Delta}{a^2}\right)^p\right], \tag{A.7}$$

$$=\frac{(D\Delta)^{l+3/2}}{\pi a^{2l+3}}\int_0^{\infty}\frac{1}{x^{4+2l}}\left[\exp\left(-x^2\right)-\sum_{p=0}^{l+1}\frac{(-1)^p}{p!}x^{2p}\right]\mathrm{d}x, \tag{A.8}$$

$$=\frac{(D\Delta)^{l+3/2}}{2\pi a^{2l+3}}\Gamma(-3/2-l), \tag{A.9}$$

$$=\frac{(D\Delta)^{l+3/2}}{2a^{2l+3}}\frac{(-1)^l}{\Gamma(5/2+l)}, \tag{A.10}$$

where $\Gamma(z)$ is the gamma function. S_1 takes finally the form

$$S_1=\frac{b\sqrt{D\Delta}}{a}\sum_{l=0}^{\infty}\frac{(l+1)(-bD)^l}{\Gamma(5/2+l)}. \tag{A.11}$$

This series reproduces the surface contribution in the signal in the form given in Eq. (13).

The part of the signal coming from the added Taylor series, S_0, consist of formal series which can be summed up exactly:

$$S_0=2\sin^2(qa)\sum_{l=0}^{\infty}(l+1)(qa)^{2l+2}\sum_{n=0}^{\infty}\frac{1}{\xi_n^{4+2l}}\times\sum_{p=0}^{l+1}\frac{(-1)^p}{p!}\left(\frac{\xi_n^2D\Delta}{a^2}\right)^p-\frac{\sin^2(qa)}{(qa)^2} \tag{A.12}$$

$$+2\cos^2(qa)\sum_{l=0}^{\infty}(l+1)(qa)^{2l+2}\sum_{n=0}^{\infty}\frac{1}{\zeta_n^{4+2l}}\sum_{p=0}^{l+1}\frac{(-1)^p}{p!}\left(\frac{\zeta_n^2D\Delta}{a^2}\right)^p,$$

$$=\exp(-bD)+O(\alpha^2). \tag{A.13}$$

To sum up the series in Eq. (A.12) it is convenient to change the summation index: $l = l_0 + p$, so that $p = 0, \ldots, \infty$ and $l_0 = -1, \ldots, \infty$. S_0 obtained in this way reproduces the first term in Eq. (12).

References

[1] T. Niendorf, R.M. Dijkhuizen, D.G. Norris, M. van Lookeren Campagne, K. Nicolay, Biexponential diffusion attenuation in various states of brain tissue: implications for diffusion-weighted imaging, Magn. Reson. Med. 36 (6) (1996) 847–857.

[2] D. Le Bihan, P. van Zijl, Editorial: from the diffusion coefficient to the diffusion tensor, NMR Biomed. 15 (2002) 431–434.

[3] C. Clark, D. Le Bihan, Water diffusion compartmentation and anisotropy at high b-values in the human brain, Magn. Reson. Med. 44 (2000) 852–859.

[4] C. Landis, X. Li, F. Telang, P. Molina, I. Palyka, G. Vetek, C. Springer, Equilibrium transcytolemma water-exchange kinetics in skeletal muscle in vivo, Magn. Reson. Med. 42 (1999) 467–478.

[5] C. Landis, X. Li, F. Telang, J. Coderre, P. Micca, W. Rooney, G. Latour, L. Lan Vetek, I. Palyka, C. Springer, Determination of the MRI contrast agent concentration time course in vivo following bolus injection: effect of equilibrium transytolemma water exchange, Magn. Reson. Med. 44 (2000) 563–574.

[6] J. Lee, C. Springer, Effects of equilibrium exchange on diffusion-weighted NMR signals: the diffusigraphic "shutter-speed", Magn. Reson. Med. 49 (2003) 450–458.

[7] L.L. Latour, K. Svoboda, P.P. Mitra, C.H. Sotal, Time-dependent diffusion of water in a biological model system, Proc. Natl. Acad. Sci. USA 91 (1994) 1229–1233.

[8] A. Schwarcz, P. Bogner, P. Meric, J. Correze, Z. Berente, J. Pal, F. Gallyas, T. Doczi, B. Gillet, J. Beloeil, The existence of biexponential signal decay in magnetic resonance diffusion-weighted imaging appears to be independent of compartmentalization, Magn. Reson. Med. 51 (2004) 278–285.

[9] Z. Ababneh, H. Beloeil, C.B. Berde, G. Gambarota, S. Maier, R.V. Mulkern, Biexponential parameterization of diffusion and T2 relaxation decay curves in a rat muscle edema model: decay curve components and water compartments, Magn. Reson. Med. 54 (2005) 524–531.

[10] A.L. Sukstanskii, D.A. Yablonskiy, Effects of restricted diffusion on MR signal formation, J. Magn. Reson. 157 (2002) 95–105.

[11] A.L. Sukstanskii, J.J.H. Ackerman, D.A. Yablonskiy, Effects of barrier-induced nuclear spin magnetization inhomogeneities on diffusion-attenuated MR signal, Magn. Reson. Med. 50 (2003) 735–742.

[12] A.L. Sukstanskii, D.A. Yablonskiy, J.J.H. Ackerman, Effects of permeable boundaries on the diffusion-attenuated MR signal: insight from a one-dimensional model, J. Magn. Reson. 170 (2004) 56–66.

[13] P. Mitra, P. Sen, L. Schwartz, P. Le Doussal, Diffusion propagator as a probe of the structure of porous media, Phys. Rev. Lett. 68 (1992) 3555–3558.

[14] P.P. Mitra, P.N. Sen, M. Schwartz, Short-time behaviour of the diffusion coefficient as a geometrical probe of porous media, Phys. Rev. B 47 (14) (1993) 8565–8574.

[15] T. de Swiet, P. Sen, Decay of nuclear magnetization by bounded diffusion in a constant field gradient, J. Chem. Phys. 100 (8) (1994) 5587–5604.

[16] P. Mitra, P. Sen, Effects of microgeometry and surface relaxation on NMR pulsed-field-gradient experiments: simple pore geometries, Phys. Rev. B 45 (1) (1992) 143–153.

[17] J.E. Tanner, E.O. Stejskal, Restricted self-diffusion of protons in colloidal systems by pulsed-gradient, spin-echo method, J. Chem. Phys. 49 (1968) 1768–1777.

[18] J. Stepišnik, Analysis of NMR self-diffusion measurements by a density matrix calculation, Physica B 104 (1981) 350–364.

[19] P. Callaghan, Principles of Nuclear Magnetic Resonance Microscopy, Oxford University Press, Oxford, 1991.

[20] J. Jensen, J. Helpern, A. Ramani, H. Lu, K. Kaczynski, Diffusional kurtosis imaging: the quantification of non-gaussian water diffusion by means of magnetic resonance imaging, Magn. Reson. Med. 53 (2005) 1432–1440.

[21] J. Stepišnik, Averaged propagator of restricted motion from the Gaussian approximation of spin echo, Physica B 344 (2004) 214–223.

[22] N. van Kampen, Stochastic Processes in Physics and Chemistry, Second ed., Elsevier Science B.V., 1997.

[23] A. Frøhlich, L. Østergaard, V. Kiselev, Effect of impermeable interfaces on apparent diffusion coefficient in heterogeneous media, App. Magn. Reson. 29 (2005) 123–137.

[24] V.G. Kiselev, Y.M. Shnir, A.Y. Tregubovich, Introduction to quantum field theory, Gordon and Breach, London, 2000.

[25] Y. Cohen, Y. Assaf, High b-value q-space analyzed diffusion-weighted MRS and MRI in neuronal tissues—a technical review, NMR Biomed. 15 (2002) 516–542.

[26] Y. Song, S. Ryu, P. Sen, Determining multiple length scales in rocks, Nature 406 (2000) 178–181.

[27] D.A. Yablonskiy, G. Bretthorst, J. Ackerman, Statistical model for diffusion attenuated MR signal, Magn. Reson. Med. 50 (2003) 664–669.

[28] M. Schachter, M. Does, A. Anderson, J. Gore, Measurements of restricted diffusion using an oscillating gradient spin-echo sequence, J. Magn. Reson. 147 (2000) 232–237.

[29] M. Does, E. Parsons, J. Gore, Gradient measurements of water diffusion in normal and globally ischemic rat brain, Magn. Reson. Med. 49 (2003) 206–215.